Condensed Matter Physics, 1998, Vol. 1, No 2(14), p. 401–408

Analytic peculiarities of the polaron mass operator in the first two orders of the coupling constant

M.Tkach, O.Voitsekhivska, O.Val'

Chernivtsi State University, Department of Theoretical Physics,
2 Kotsubynsky St., UA–274012 Chernivtsi, Ukraine

Received April 25, 1998

The exact analytic expression for the polaron mass operator in the second order of the coupling constant is established for the first time. It holds in the whole energy scale. The peculiarities of the mass operator are analysed. The renormalized polaron energy spectrum is obtained and analysed in this approximation.

Key words: *polaron, mass operator, diagram technique*

PACS: *71.38.+i*

1. Introduction

Polaron as a quasiparticle was studied by Feynman, Landau, Pekar, Pines, Rashba [1] and others. Nevertheless, a lot of physical and mathematical problems have not been solved yet. As far as the physics of polaron is concerned, the most important problem concerns the existence of bound complexes [2]. The mathematical problems of the correct calculation of the electron and phonon spectra in the region of high energies, quasimomentum and electron-phonon binding are tightly connected with physical ones. There is an important question about the ranges of diagram technique convergence for the polaron Green function.

The actual problem is the analytical calculation of the polaron mass operator (MO) in the higher orders of the binding constants, because the exact numerical results are obtained only in one-phonon approximation [1-3] while the contribution of any higher order diagrams is done, as a rule, only evaluatively.

In this paper the exact analytical calculation of the polaron MO is performed for the first two orders of the coupling constant in the arbitrary range of energies at $T = 0$ K. On this basis the dependence of the renormalized energy of the polaron zone bottom on the coupling constant is derived. Some peculiarities of the MO behaviour in the region of energies higher than the phonon creation threshhold are studied.

2. Frohlich Hamiltonian. Analytic expression for $M_2(\boldsymbol{k},\boldsymbol{\omega})$

It is known that the polaron is described by the Frohlich Hamiltonian [1]

$$H=\sum_{\boldsymbol{k}} E_{\boldsymbol{k}} a_{\boldsymbol{k}}^{+} a_{\boldsymbol{k}}+\sum_{\boldsymbol{q}} \Omega_{\boldsymbol{q}}(b_{\boldsymbol{q}}^{+} b_{\boldsymbol{q}}+1/2)+\sum_{\boldsymbol{k},\boldsymbol{q}} \varphi_{\boldsymbol{q}} a_{\boldsymbol{k}+\boldsymbol{q}}^{+} a_{\boldsymbol{k}}(b_{\boldsymbol{q}}+b_{\boldsymbol{q}}^{+}), \tag{1}$$

where $E_{\boldsymbol{k}}=E+\frac{\hbar^2 k^2}{2m}; \Omega_{\boldsymbol{q}}=\omega; \varphi(\boldsymbol{q})=\frac{\alpha}{q}$ are the dispersion laws of the electron and optical phonons, respectively, and their binding function is expressed within the Frohlich constant

$$\alpha=\frac{e^2}{\hbar}\left(\frac{1}{\epsilon_\infty}-\frac{1}{\epsilon_0}\right)\sqrt{\frac{m}{2\Omega}}. \tag{2}$$

At $T=0$ K the renormalization of the electron-phonon spectrum is defined by the polaron Green function Fourier image poles. It is given by the Dyson equation

$$G(\boldsymbol{k},\omega')=\frac{1}{\omega-\varepsilon-M(\boldsymbol{k},\omega)} \tag{3}$$

with the total MO given by an infinite range of diagrams [4].

The expression for the first diagram corresponding to one-phonon approximation reads:

$$M_2(\boldsymbol{k},\omega')=\sum_{\boldsymbol{q}}\frac{\varphi^2(\boldsymbol{q})}{\omega-E_{\boldsymbol{k}+\boldsymbol{q}}-\Omega}. \tag{4}$$

Introducing the convenient dimensionless quantities

$$m_2=\frac{M_2}{\Omega},\quad \xi=\omega-\frac{E}{\Omega},\quad \boldsymbol{K}=\frac{\hbar}{\sqrt{2m\Omega}}\boldsymbol{k},\quad \boldsymbol{Q}=\frac{\hbar}{\sqrt{2m\Omega}}\boldsymbol{q} \tag{5}$$

one can obtain

$$m_2(\boldsymbol{K},\xi')=\frac{\alpha}{2\pi^2}\int_{-\infty}^{\infty}\frac{\mathrm{d}^3Q}{Q^2[\xi-1-(\boldsymbol{K}-\boldsymbol{Q})^2]}. \tag{6}$$

Integration in (6) can be performed exactly and gives the known [2,3] result:

$$m_2(K,\xi')=-\frac{\alpha}{K}\begin{cases}\arctan\frac{K}{\sqrt{1-\xi}}, & \xi<1,\\ \frac{i}{2}\ln\left|\frac{\sqrt{1-\xi}-K}{\sqrt{1-\xi}+K}\right|, & \xi>1.\end{cases} \tag{7}$$

At $K=0$ one can get

$$\mathfrak{Re}\;\; m_2(\xi)=\begin{cases}-\frac{\alpha}{\sqrt{1-\xi}}, & \xi<1,\\ 0, & \xi>1,\end{cases} \tag{8}$$

$$\mathfrak{Im}\;\; m_2(\xi)=\begin{cases}0, & \xi>1,\\ \frac{\alpha}{\sqrt{1-\xi}}, & \xi<1.\end{cases} \tag{9}$$

Analytical expressions for one-phonon MO give an opportunity to study the renormalized polaron spectrum in this approximation.

3. Analytical calculation of $M_4^a(\boldsymbol{k},\boldsymbol{\omega})$

MO of the fourth order in the powers of the binding function which corresponds to the diagrams without crossing the phonon lines [1,4] is defined as

$$M_4^a(\boldsymbol{k},\omega)=\sum_{\boldsymbol{q_1},\boldsymbol{q_2}}\frac{\varphi^2(\boldsymbol{q_1})\varphi^2(\boldsymbol{q_2})}{(\omega-\varepsilon_{\boldsymbol{k}+\boldsymbol{q_1}}-\Omega)^2(\omega-\varepsilon_{\boldsymbol{k}+\boldsymbol{q_1}+\boldsymbol{q_2}}-2\Omega)}, \tag{10}$$

according to the rules of a diagram technique. Performing in (10) a transition from summation to integration with taking into account the dispersion laws, binding functions and by introducing the dimensionless quantities, (10) one can obtain

$$m_4^a(\boldsymbol{K},\xi)=\frac{\alpha^2}{4\pi^4}\int\limits_{-\infty}^{\infty}\frac{\mathrm{d}^3Q_1}{Q_1^2[\xi-1-(\boldsymbol{K}+\boldsymbol{Q_1})^2]}\int\limits_{-\infty}^{\infty}\frac{\mathrm{d}^3Q_2}{Q_2^2[\xi-2-(\boldsymbol{K}+\boldsymbol{Q_1}+\boldsymbol{Q_2})^2]}. \tag{11}$$

Integration in (11) is performed in the spherical coordinate system. Herein, in the internal integrals θ_2 is the angle between vectors $\boldsymbol{K}+\boldsymbol{Q_1}$ and $\boldsymbol{Q_2}$ and in the external integrals θ_1 is the angle between $\boldsymbol{K}$ and $\boldsymbol{Q_1}$. Insertion of $\cos\theta_1=x_1$ and $\cos\theta_2=x_2$ and integration over the angles φ_1 and φ_2 give the following result:

$$\begin{aligned}m_4^a(\boldsymbol{K},\xi)=\frac{\alpha^2}{\pi^2}\int\limits_{-1}^{1}\mathrm{d}x_1\int\limits_{0}^{\infty}\frac{\mathrm{d}Q_1}{[\xi-1-(K^2+2KQ_1x_1+Q_1^2)]^2}\times\\ \times\int\limits_{-1}^{1}\mathrm{d}x_2\int\limits_{0}^{\infty}\frac{\mathrm{d}Q_2}{\xi-2-[(\boldsymbol{K}+\boldsymbol{Q_1})^2+2(\boldsymbol{K}+\boldsymbol{Q_1})\boldsymbol{Q_2}x_2+Q_2^2]}.\end{aligned} \tag{12}$$

Two internal integrals in (12) are taken in a general case and the results read:

$$\begin{aligned}m_4^a(\boldsymbol{K},\xi)=-\frac{\alpha^2}{\pi}\int\limits_{-1}^{1}\mathrm{d}x_1\int\limits_{0}^{\infty}\frac{\mathrm{d}Q_1}{\sqrt{K^2+2KQ_1x_1+Q_1^2}[\xi-1-(K^2+2KQ_1x_1+Q_1^2)]}\times\\ \begin{cases}\arctan\sqrt{\frac{K^2+2KQ_1x_1+Q_1^2}{2-\xi}}, & \xi<2,\\ \frac{i}{2}\ln\left|\frac{\sqrt{2-\xi}-\sqrt{K^2+2KQ_1x_1+Q_1^2}}{\sqrt{2+\xi}+\sqrt{K^2+2KQ_1x_1+Q_1^2}}\right|, & \xi>2.\end{cases}\end{aligned} \tag{13}$$

As at $K\neq 0$ integrating in (13) cannot be performed exactly, then $m_4^a(\xi,K=0)$ can be calculated. From (13) it is clear that in the $\xi<1$ region $m_4^a(\xi<1)$ is a real function of variable ξ and is given by the expression

$$m_4^a(\xi<1)=-\frac{2\alpha^2}{\pi}\int\limits_{0}^{\infty}\frac{\mathrm{d}Q_1\arctan Q_1(\sqrt{2-\xi})^{-1}}{Q_1(1-\xi+Q_1^2)}. \tag{14}$$

Using

$$\frac{1}{(1-\xi+Q_1^2)^2}=-\lim_{\tau\to 1-\xi}\frac{d}{d\tau}(\tau+Q_1^2)^{-1} \tag{15}$$

and taking into account the known integral [5]

$$I(q,p) = \int\limits_0^\infty \arctan(qx) \frac{\mathrm{d}x}{x(p^2+x^2)} = \frac{\pi}{2p^2} \ln(1+qp), (p>0, q \geqslant 0) \tag{16}$$

from (16) the expression for $m_4^a(\xi < 1)$ containing only the real part can be obtained

$$m_4^a(\xi<1) = -\frac{\alpha^2}{(1-\xi)^2}\left[\ln\left(1+\sqrt{\frac{1-\xi}{2-\xi}}\right) - \frac{\sqrt{1-\xi}}{2(\sqrt{1-\xi}+\sqrt{2-\xi})}\right]. \tag{17}$$

The analytical continuation of (17) into the region $1 < \xi < 2$ gives the real and imaginary parts

$$m_4^a(1<\xi<2) = \frac{\alpha^2}{(\xi-1)^2}\left\{\frac{\xi-1}{2} + \ln(2-\xi) + i\left[\frac{\sqrt{(\xi-1)(2-\xi)}}{2} - \arctan\sqrt{\frac{\xi-1}{2-\xi}}\right]\right\}, \tag{18}$$

and extending (17) into the region $\xi > 2$ gives only the real part

$$m_4^a(2<\xi) = -\frac{\alpha^2}{(\xi-1)^2}\left[\ln\left(1+\sqrt{\frac{\xi-1}{\xi-2}}\right) - \frac{\sqrt{\xi-1}}{2(\sqrt{\xi-1}+\sqrt{\xi-2})}\right]. \tag{19}$$

Finally, formulas (17)-(19) completely define $m_4^a(\xi)$ as a complex function of the real dimensionless energy ξ in the whole region of its variation.

4. Analytical calculation of $M_4^b(\boldsymbol{k},\boldsymbol{\omega})$

The expression for the MO diagram of the fourth order with the crossing of phonon lines reads:

$$M_4^b(\boldsymbol{k},\omega) = \sum_{\boldsymbol{q_1},\boldsymbol{q_2}} \frac{\varphi^2(\boldsymbol{q_1})\varphi^2(\boldsymbol{q_2})}{(\omega-\varepsilon_{\boldsymbol{k}+\boldsymbol{q_1}}-\Omega)(\omega-\varepsilon_{\boldsymbol{k}+\boldsymbol{q_2}}-\Omega)(\omega-\varepsilon_{\boldsymbol{k}+\boldsymbol{q_1}+\boldsymbol{q_2}}-2\Omega)}. \tag{20}$$

Using the dimensionless variables one can obtain

$$m_4^b(\boldsymbol{K},\xi) = \frac{\alpha^2}{4\pi^4}\int\limits_{-\infty}^{\infty}\frac{\mathrm{d}^3\boldsymbol{Q_1}}{Q_1^2[\xi-1-(\boldsymbol{K}+\boldsymbol{Q_1})^2]}\int\limits_{-\infty}^{\infty}\frac{\mathrm{d}^3\boldsymbol{Q_2}}{Q_2^2[\xi-1-(\boldsymbol{K}+\boldsymbol{Q_2})^2][\xi-2-(\boldsymbol{K}+\boldsymbol{Q_1}+\boldsymbol{Q_2})^2]}. \tag{21}$$

At arbitrary K exact integration cannot be performed. At $K=0$ one can pass to the spherical coordinate system in both integrals. Herein, θ_2 is the angle between vectors $\boldsymbol{Q_1}$ and $\boldsymbol{Q_2}$. Insertion of $\cos\theta_2 = x$ and integration over the angles φ_1, φ_2 and θ_2 gives the following result for $m_4^b(\xi)$:

$$m_4^b(\xi) = \frac{2\alpha^2}{\pi^2}\int\limits_0^\infty\frac{\mathrm{d}Q_1}{\xi-1-Q_1^2}\int\limits_{-1}^{1}\mathrm{d}x\int\limits_0^\infty\frac{\mathrm{d}Q_2}{(\xi-1-Q_2^2)[\xi-2-(Q_1^2+2Q_1Q_2x+Q_2^2)]}. \tag{22}$$

From equation (22) it is clear that in the region $\xi < 1$ the internal double integral has not any peculiarities. Using the integral

$$\begin{aligned} I(t,\alpha,a,K) = -\int_{-1}^{1}\mathrm{d}x\int_{0}^{\infty}\tfrac{\mathrm{d}Q}{(t+\alpha Q^2)(a+K^2+2KQx+Q^2)} = \\ = \tfrac{\pi}{2Kt}\left\{\arctan\tfrac{K}{\sqrt{a}} + \arctan\left[\tfrac{K}{\sqrt{a}}\tfrac{t+\alpha(K^2+a)}{t-\alpha(K^2+a)}\right] - \arctan\left[\tfrac{2K\sqrt{\alpha t}}{t-\alpha(K^2+a)}\right]\right\} \end{aligned} \quad (23)$$

for m_4^b in the region $\xi < 1$ the following expression is obtained:

$$\begin{aligned} m_4^b(\xi<1) = -\tfrac{\alpha 2}{\pi(1-\xi)}\int_0^{\infty}\tfrac{\mathrm{d}Q_1}{Q_1(Q_1+1-\xi)}\times \\ \times\left[\arctan\tfrac{Q_1}{\sqrt{2\xi}} + \arctan\left(\tfrac{2Q_1\sqrt{1-\xi}}{1+Q_1^2}\right) - \arctan\left(\tfrac{Q_1}{\sqrt{2-\xi}}\tfrac{Q_1^2+3-2\xi}{1+Q_1^2}\right)\right]. \end{aligned} \quad (24)$$

Integration in (24) can be performed exactly when the arguments of all the arctan functions are linear in Q. Using the expression

$$\arctan(\frac{2Q_1\sqrt{1-\xi}}{1+Q_1^2}) = \arctan[(\sqrt{1-\xi}+\sqrt{2-\xi})x] - \arctan\left(\frac{x}{\sqrt{1-\xi}+\sqrt{2-\xi}}\right) \quad (25)$$

the last term of (25) can be written in the form:

$$\begin{aligned} \arctan\left(\tfrac{Q_1}{\sqrt{2-\xi}}\tfrac{Q_1^2+3-2\xi}{1+Q_1^2}\right) = \arctan\alpha_1 Q_1 + \arctan\alpha_2 Q_1 + \arctan\alpha_3 Q_1 = \\ = \arctan\left[-\tfrac{Q_1^3\alpha_1\alpha_2\alpha_3 - Q_1(\alpha_1+\alpha_2+\alpha_3)}{1-Q_1^2(\alpha_1\alpha_2+\alpha_1\alpha_3+\alpha_2\alpha_3)}\right]. \end{aligned} \quad (26)$$

The result of the integration reads:

$$\begin{aligned} m_4^b(\xi<1) = -\tfrac{\alpha 2}{2(1-\xi)^2}\{\ln\left[\tfrac{(\sqrt{2-\xi}+\sqrt{1-\xi})^3}{\sqrt{2-\xi}+2\sqrt{1-\xi}}\right] - \ln[1+(\alpha_1+\alpha_2+\alpha_3)\sqrt{1-\xi}+ \\ +(\alpha_1\alpha_2+\alpha_1\alpha_3+\alpha_2\alpha_3)(1-\xi)+\alpha_1\alpha_2\alpha_3\sqrt{1-\xi}^3]\}. \end{aligned} \quad (27)$$

Combinations of the coefficients $\alpha_1, \alpha_2, \alpha_3$ can be obtained from the (26) formula and, obviously,

$$\alpha_1\alpha_2\alpha_3 = -\frac{1}{\sqrt{2-\xi}}, \quad \alpha_1\alpha_2+\alpha_1\alpha_3+\alpha_2\alpha_3 = -1, \quad \alpha_1+\alpha_2+\alpha_3 = \frac{3-2\xi}{\sqrt{2-\xi}}. \quad (28)$$

Inserting (28) into (27) one can get an analytical expression for $m_4^b(\xi < 1)$ as a real function on ξ in this region

$$m_4^b(\xi<1) = -\frac{\alpha^2}{2(1-\xi)^2}\ln\frac{(\sqrt{2-\xi}+\sqrt{1-\xi})^3}{(\sqrt{2-\xi}+2\sqrt{1-\xi})[\sqrt{(1-\xi)(2-\xi)}+\xi]}. \quad (29)$$

The analytic continuation of (29) into the region $1 < \xi < 2$ gives both real and imaginary parts

$$m_4^b(1<\xi<2) = \frac{\alpha^2}{(\xi-1)^2}\left[\frac{1}{2}\ln(3\xi-2) - i\arctan\left(\frac{2(\xi-1)}{2\xi-1}\sqrt{\frac{\xi-1}{2-\xi}}\right)\right] \quad (30)$$

and analytic continuation of (29) into the region $\xi > 2$ gives only the real part

$$m_4^b(\xi > 2) = -\frac{\alpha^2}{2(1-\xi)^2} \ln\left[\frac{(\sqrt{\xi-2}+\sqrt{\xi-1})^2}{3\xi-2}\right]. \tag{31}$$

Finally, formulas (29)-(31) completely define $m_4^b(\xi)$ as a complex function on the real variable ξ in the whole range of its variation.

5. Analysis of the results

Figures 1a, 1b show the frequency dependences of the MO terms (real and imaginary) calculated by the formulas obtained in the previous sections at $\alpha = 1$. From the figures one can see:

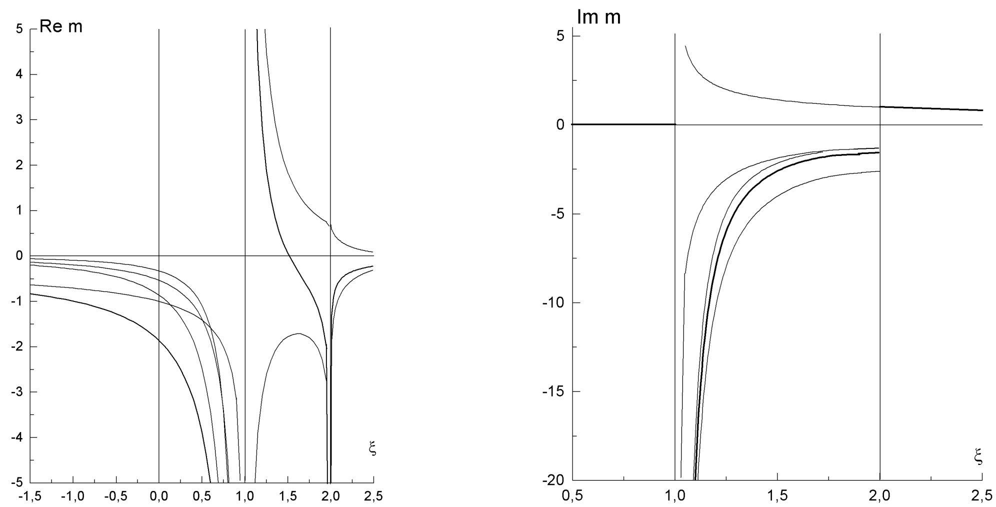

Figure 1. Dependence of the terms $\Re\mathfrak{e}\ m$ (figure 1a) and $\Im\mathfrak{m}\ m$ (figure 1b) on ξ at $\alpha = 1$. Thin solid curve corresponds to m_2, dotted - m_4^a, dashed - m_4^b, dashed-dotted - $m_4^a + m_4^b$, thick solid - $m_2 + m_4^a + m_4^b$, respectively.

In the energy region $\xi \leqslant 1$ all the three terms of MO (m_2, m_4^a, m_4^b) are real and negative independently of the α magnitude. Herein, $|m_4^a| < |m_4^b|$ and only when ξ reaches value 1 from the left-hand side, the relation holds $m_4^a \sim m_4^b \sim -\frac{\alpha^2}{2(1-\xi)^{\frac{3}{2}}}$. As far as near this point $m_2 \sim -\frac{\alpha}{\sqrt{1-\xi}}$ then

$$\lim_{\xi\to 1+\varepsilon} \frac{m_4^a(\xi)+m_4^b(\xi)}{m_2(\xi)} \sim -\lim_{\xi\to 1-\varepsilon} \frac{\alpha}{1-\xi} = -\frac{\alpha}{\varepsilon}. \tag{32}$$

So, in the region $\xi \leqslant 1$ MO diagrams of order α^2 have a bigger discrepancy than one-phonon diagrams. Therefore, one has to consider more than the first three diagrams in the total MO. The region where the account of the first three MO diagrams is not enough can be evaluated from the condition $\xi' < \xi < 1$ where ξ' is the solution of the equation

$$m_2(\xi') = m_4^a(\xi') + m_4^b(\xi'). \tag{33}$$

It is clear that the bigger is α magnitude the bigger is the region. When $\xi' < \xi$, this approximation is correct.

In the $1 \leqslant \xi \leqslant 2$ energy region $\mathfrak{Re}\, m_2 = 0$, $\mathfrak{Re}\, m_4^a < 0$, $\mathfrak{Re}\, m_4^b > 0$. Herein, as $\mathfrak{Re}\, m_4^a|_{\xi\to 1+\varepsilon} \sim \frac{\alpha^2}{2(\xi-1)}$, $\mathfrak{Re}\, m_4^b|_{\xi\to 1+\varepsilon} \sim \frac{3\alpha^2}{2(\xi-1)}$, then

$$\mathfrak{Re}\,(m_2 + m_4^a + m_4^b)\Big|_{\xi\to 1+\varepsilon} \sim \frac{\alpha^2}{\xi - 1}\Big|_{\xi\to 1+\varepsilon} \sim \frac{\alpha^2}{\varepsilon} \to +\infty. \tag{34}$$

In the $\xi \to 2\varepsilon$ region $\mathfrak{Re}\, m_4^a(\xi) \sim \alpha^2 \ln\varepsilon \to -\infty$, $\mathfrak{Re}\, m_4^b(\xi) \sim \alpha^2 \ln 2$, then

$$\mathfrak{Re}\,(m_2 + m_4^a + m_4^b)|_{\xi\to 2\varepsilon} \sim \alpha^2 \ln\varepsilon \to -\infty. \tag{35}$$

So, independently of the α magnitude in the region $1 \leqslant \xi \leqslant 2$, function $\mathfrak{Re}\,[m_2(\xi) + m_4^a(\xi) + m_4^b(\xi)]$ has the same qualitative dependence on ξ as it is shown in figure 1a.

It is clear from the analytical expressions and from figure 1b that in the $1 \leqslant \xi \leqslant 2$ energy region $\mathfrak{Im}\, m_2 > 0$, $\mathfrak{Im}\, m_4^a < 0$, $\mathfrak{Im}\, m_4^b < 0$. Herein,

$$\begin{aligned} \mathfrak{Im}\, m_2(\xi \to 1+\varepsilon) &\sim \tfrac{\alpha}{\sqrt{\xi-1}} \sim \tfrac{\alpha}{\sqrt{\varepsilon}} \sim \infty, \\ \mathfrak{Im}\, m_4^a(\xi \to 1+\varepsilon) &\sim -\tfrac{\alpha^2}{2(\xi-1)^{\frac{3}{2}}} \sim -\tfrac{\alpha^2}{2\varepsilon^{\frac{3}{2}}} \sim -\infty, \\ \mathfrak{Im}\, m_4^b(\xi \to 1+\varepsilon) &\sim -\tfrac{2\alpha^2}{\sqrt{\xi-1}} \sim -\tfrac{2\alpha^2}{\sqrt{\varepsilon}} \sim -\infty. \end{aligned} \tag{36}$$

As in the region $\xi \to 1+\varepsilon$ holds $|\,\mathfrak{Im}\,(m_4^a + m_4^b)| > |\,\mathfrak{Im}\, m_2|$, then $\mathfrak{Im}\,(m_2 + m_4^a + m_4^b) < 0$, which proves that the first three MO diagrams give incorrect results in this energy region.

It is clear from figure 1b that at rather small $\alpha(\alpha \ll 1)$ values in the $1 \leqslant \xi \leqslant 2$ energy region the condition $\mathfrak{Im}\,[m_2(\xi) + m_4^a(\xi) + m_4^b(\xi)] > 0$ can be satisfied. Herein, in the same region the condition

$$\xi - \mathfrak{Re}\,(m_2 + m_4^a + m_4^b) = 0 \tag{37}$$

is satisfied, too, meaning the possibility of the existence of a strongly damped bound state in the electron-phonon system (one-phonon repetition).

In the region $\xi > 2$ all the three terms of MO are completely defined and their frequency dependence is given in figures 1a,b. It is not to be analysed in detail because it is clear that in this energy region the MO terms of α^3 order play a significant role.

Figure 2 shows the dependence of the renormalized energy module ($|\xi_0|$) on the coupling constant α calculated within the dispersional equation

$$\xi - \mathfrak{Re}\, m(\xi) = 0 \tag{38}$$

in linear (dotted curve) and square (dased curve) approximations. The dependence which is true in the region of weak and intermediate coupling q (known from literature [1]) is presented. Figure 2 proves that a diagram of the first order (α^1) gives satisfactory results only at $\alpha \leqslant 0.4$. Taking into account both diagrams of the second order in the region ($\alpha \leqslant 0.9$) gives even better results than all other theories [1]. In the region $\alpha > 1$ these terms make the magnitude of the renormalized energy obtained in one-phonon approximation much more exact.

The obtained peculiarities of the MO behaviour in the vicinity of $\xi = 1$ show an important role of MO diagrams of a higher order and not only those having "dangerous crossings" [2]. The analysis of this problem is to be made in future taking into account partially summed infinite series of MO diagrams.

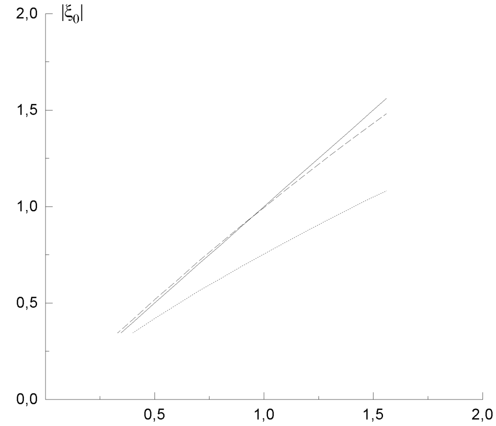

Figure 2. Dependence of the polaron zone bottom shift on α.

References

1. Firsov Ju.A. Polarons. Moscow, Nauka, 1975 (in Russian).
2. Levinson Y.B., Rashba E.I. Threshold phenomena and bound states in polaron probleme. // Uspehi Fiz. Nauk, 1973, vol. 111, No 4, p. 683-718 (in Russian).
3. Klochihin A.A. Spectrum of free polaron and radius of perturbation theory. // Fiz. Tverd. Tela, 1979, vol. 21, No 10, p. 3077-3085 (in Russian).
4. Abrikosov A.A., Gorkov L.P., Dzyaloshinski I.E. Methods of quantum field theory in statistical physics. Dover Publ., New York, 1975.
5. Gradshtein I.S., Ryzhik I.M. Tables of integrals, sums, serieses and multiplies. Moscow, Fizmatgiz, 1962.

Аналітичні властивості масового оператора полярона в перших двох порядках за константою зв'язку

М.Ткач, О.Войцехівська, О.Валь

Чернівецький державний університет, кафедра теоретичної фізики
274012 м. Чернівці, вул. Коцюбинського, 2

Отримано 25 квітня 1998 р.

Вперше отримано точний аналітичний вираз для масового оператора полярона у другому порядку за константою зв'язку, справедливий для всієї області енергій. Проаналізовано особливості масового оператора. Знайдено і проаналізовано перенормований енергетичний спектр полярона у цьому наближенні.

Ключові слова: *полярон, масовий оператор, діаграмна техніка*

PACS: *71.38.+i*